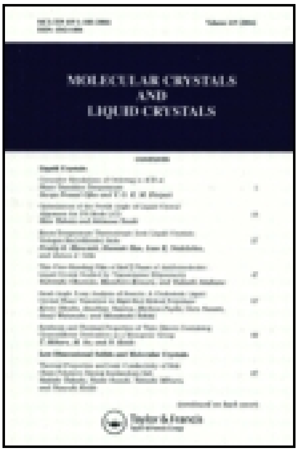

Molecular Crystals and Liquid Crystals
Publication details, including instructions for authors and subscription information:
http://www.tandfonline.com/loi/gmcl20

Synthesis, Characterization and Mesomorphic Properties of Unsymmetrical N-[4-(Alkoxy)-2-Hydroxybenzylidene]-N′-(4-Alkoxybenzylidene) Azines and Their Copper (II) Complexes

Ashwini Pandey [a] & Bachcha Singh [a]

[a] Department of Chemistry (Centre of Advanced Study), Faculty of Science, Banaras Hindu University, Varanasi, Uttar Pradesh, India

To cite this article: Ashwini Pandey & Bachcha Singh (2012): Synthesis, Characterization and Mesomorphic Properties of Unsymmetrical N-[4-(Alkoxy)-2-Hydroxybenzylidene]-N′-(4-Alkoxybenzylidene) Azines and Their Copper (II) Complexes, Molecular Crystals and Liquid Crystals, 552:1, 123-133

To link to this article: http://dx.doi.org/10.1080/15421406.2011.607323

Mol. Cryst. Liq. Cryst., Vol. 552: pp. 123–133, 2012

ISSN: 1542-1406 print/1563-5287 online
DOI: 10.1080/15421406.2011.607323

Synthesis, Characterization and Mesomorphic Properties of Unsymmetrical N-[4-(Alkoxy)-2-Hydroxybenzylidene]-N′-(4-Alkoxybenzylidene) Azines and Their Copper (II) Complexes

ASHWINI PANDEY AND BACHCHA SINGH*

Department of Chemistry (Centre of Advanced Study), Faculty of Science,
Banaras Hindu University, Varanasi, Uttar Pradesh, India

A new series of mesogenic unsymmetrical azines, N-[4-(alkoxy)-2-hydroxybenzylidene]-N′-(4-n-alkoxybenzylidene) azines, $ROC_6H_4CH{=}N{-}N{=}CHC_6H_3OHOR$, where $R{=}C_mH_{2m+1}$ (m = 6, 8, 10, 12, and 14), and their copper (II) complexes has been synthesized. They were characterized by elemental analyses, Fourier transform infrared (FT-IR), ^1H and ^{13}C nuclear magnetic resonance (NMR) spectra, ultraviolet (UV)-visible, and magnetic susceptibility measurements. The copper (II) complexes are square planar. The mesomorphic properties of these compounds were investigated by differential scanning calorimetry and polarizing microscopy. The unsymmetrical azines with m = 6, 12, and 14 exhibit monotropic nematic, enantiotropic, and monotropic smectic A phases, whereas azines with m = 8 display enantiotropic nematic and m = 10 display both enantiotropic smectic A and nematic mesophases in the heating and cooling cycles. The copper (II) complexes of the azines are nonmesomorphic in nature with high clearing temperatures and displayed polymorphism (crystal–crystal transitions) in both the heating and cooling cycles.

Keywords Differential scanning calorimetry; enantiotropic nematic mesophase; enantiotropic smectic A phase; monotropic nematic phase; polarizing optical microscopy

1. Introduction

Azine molecules possess interesting physicochemical properties. They have increased interest for their potential in medical and biological applications [1,2], in the design of metal complexes [3,4], and other materials applications [5,6].

Iwan et al. [7] reported liquid crystalline phases formed by symmetrical azines with different terminal alkoxy semiperfluorinated end groups, which exhibit the smectic C (SmC) phase, whereas azines with octadecyloxy end chains showed SmC and SmA phases. Azines with 5″-octyl-2,2′,5′,2″-terthiophene groups exhibit only a nematic phase. Different types of nematic and SmC textures were found and investigated by polarizing optical microscopy. Besides liquid crystalline properties, azines also exhibit photoluminescence and thermoluminescence properties.

---

*Address correspondence to Bachcha Singh, Department of Chemistry (Centre of Advanced Study), Faculty of Science, Banaras Hindu University, Varanasi 221005, Uttar Pradesh, India. E-mail: bsinghbhu@rediffmail.com

We have also reported a new series of mesogenic unsymmetrical azines [8], N-(*o*-hydroxybenzylidene)-N′-(4-*n*-alkoxybenzoyloxybenzylidene) azines, with terminal alkoxy chain lengths of 7–16. $HOC_6H_4CH{=}N{-}N{=}CHC_6H_4COC_6H_4OC_mH_{2m+1}$ in which the azines with $m = 7$, 10, and 14 exhibit an enantiotropic nematic (N) mesophase, whereas azines with $m = 8$ and 11 exhibit a monotropic nematic phase. Ligands with $m = 9$ and 12 displayed no mesomorphic behavior. Furthermore, we have also reported [9] another series of mesogenic unsymmetrical azines, N-(*o*-hydroxybenzylidene)-N′-(4-*n* alkoxybenzylidene) azines, $HOC_6H_4CH{=}N{-}N{=}CHC_6H_4OC_mH_{2m+1}$ ($m = 6$–16) and their copper (II) complexes. The mesomorphic properties of these compounds were investigated by differential scanning calorimetry (DSC) and polarizing optical microscopy. All of the unsymmetrical azines, except $m = 7$, exhibit mesomorphism. The azine with $m = 8$ shows a monotropic nematic mesophase, whereas all other azines exhibit an SmA mesophase in the cooling cycle. The copper (II) complexes of the azines show only an isotropic phase at higher temperatures ($\sim$180°C) and no mesomorphism is observed.

It was thought worthwhile to synthesize a new series of liquid crystalline unsymmetrical azines, N-[4-(alkoxy)-2-hydroxybenzylidene]-N′-(4-alkoxybenzylidene) azines, because of their interesting liquid crystalline behavior over a broad thermal range of nematic and smectic phases. The characterization details and the result of the investigations based on DSC and polarizing optical microscopy are reported in this article.

2. Experimental Details

2.1 Materials

2,4-Dihydroxybenzaldehyde, 4-hydroxybenzaldehyde, 1-bromoalkanes, hydrazine monohydrate, potassium carbonate, potassium iodide, and copper acetate monohydrate were purchased from Aldrich Chemicals (St. Louis, MO, USA) and used as received. All other solvents and reagents were purchased commercially and used after purification.

2.2 Techniques

Elemental analyses were performed on a CE440 Exeter Analytical CHN analyzer. Infrared (IR) spectra were recorded on a Fourier transform infrared (FT-IR) Varian 3100 Excalibur series spectrophotometer in KBr pellets in the 4000–100 cm^{-1} region. ^1H and ^{13}C nuclear magnetic resonance (NMR) spectra were obtained on a JEOL FT-NMR AL (300 MHz) spectrometer using tetramethyl silane as the internal standard. Electronic spectra were recorded on an ultraviolet (UV)-1700 Pharma Spec.Shimadzu UV-visible spectrophotometer. Magnetic susceptibility measurements at room temperature were carried out on a Cahn–Faraday balance using $Hg[Co(NCS)_4]$ calibrant, and the experimental magnetic susceptibilities were corrected for diamagnetism using Pascal's constants. DSC thermograms were recorded with a Mettler Toledo TC15 TA differential scanning calorimeter at the rate of 10.0 K min^{-1} under a nitrogen atmosphere using spec pure grade zinc and indium as standards by taking samples in closed-lid aluminum pans. The transition temperatures from DSC have been determined with an accuracy of ±0.1 K. The mesophase type exhibited by the compounds was identified by visual comparison with known phase standards using an HT 30.01 NTT 268 Lomo polarizing optical microscope fitted with a hot stage with a temperature controlling accuracy of 0.1 K. The copper content in the complex was determined using an atomic absorption spectrophotometer (ASH Corp.).

2.3 Synthesis of Compounds

*2.3.1 Synthesis of 4-n-Alkoxybenzaldehydes (**2**).* The synthesis of 4-*n*-alkoxy benzaldehydes (**2**), namely, 4-hexyloxy-, 4-heptyloxy-, 4-decyloxy-, 4-dodecyloxy-, and 4-tetradecyloxybenzaldehydes was carried out as described earlier [10].

*2.3.2 Synthesis of 4-Decyloxybenzhydrazone (**3c**).* To an ice-cold ethanolic solution (10 ml) of hydrazine hydrate (0.49 g, 10 mmol), an ethanolic (10 ml) solution of 4-decyloxybenzaldehyde (2.62 g, 10 mmol) was added dropwise with continuous stirring. The reaction mixture was then immediately evaporated on a rotavapor to yield a white residue. This was washed with water, dried, and recrystallized from chloroform. Yield: 70%. FT-IR (KBr, cm^{-1}): 3381ν_a (N—H), 3284 ν_S (N—H), 2934, 2861 (aliphatic C—H), 1632 (C=N), 1601, 1505 (Ph), 1308, 1260 (OPh), 1031 (N—N). ^{1}H NMR ($CDCl_3$, TMS) δ_H (ppm): 7.87 (s, 1H, —CH=N), 7.84–6.88 (d, 4H, ArH), 5.42 (s, 2H, $-NH_2$), 4.06–4.01 (t, 2H, $-OCH_2$), 2.36–1.31 (m, 16H, $[CH_2]_n$), 0.88 (t, 3H, $-CH_3$).

All other members of the homologous series, namely, 4-hexyloxy-, 4-heptyloxy-, 4-dodecyloxy-, and 4-tetradecyloxy benzhydrazones, were prepared using the above procedure.

*2.3.3 Synthesis of 4-n-Decyloxy-2-Hydroxybenzaldehyde (**5c**).* To a solution of 2,4-dihydroxybenzaldehyde (**4**) (0.138 g, 10 mmol) in 35 ml of ethanol, 1-bromodecane (4.4 ml, 22 mmol), K_2CO_3 (3.36 g, 22 mmol), and KI in catalytic amount were added. The reaction mixture was heated under reflux for 36 h. After cooling, the reaction mixture was filtered out. The filtrate was neutralized by dilute HCl and further 40 ml of distilled water was added. The aqueous layer was extracted thrice with 30 ml portions of chloroform. The chloroform extract was combined and dried over anhydrous $MgSO_4$. On evaporation it gave 2-hydroxy-4-(decyloxy)benzaldehyde as yellow oil in 53% yield. ^{1}H NMR ($CDCl_3$, TMS) δ_H (ppm): 11.48 (s, 1H, —OH), 9.69 (s, 1H, —CHO), 7.80 (d, 1H, ArH), 6.51 (d, 1H, ArH), 6.41 (s, 1H, ArH), 4.04 (t, 2H, $-OCH_2$), 2.21–1.13 (m, 16H, $-[CH_2]_n$), 0.88 (t, 3H, $-CH_3$).

All other members of the homologous series, namely, 4-(hexyloxy)-, 4-(heptyloxy)-, 4-(dodecyloxy)-, and 4-(tetradecyloxy)-2-hydroxybenzaldehydes, were prepared using the above procedure.

*2.3.4 Synthesis of N-[4-(Decyloxy)-2-Hydroxybenzylidene]-N′-(4-Decyloxybenzylidene) Azine (**6c**).* To a solution of 4-decyloxybenzhydrazone (1.31 g, 5 mmol) in chloroform (25 ml), a solution of 4-(decyloxy)-2-hydroxybenzaldehyde (1.39 g, 5 mmol) in chloroform along with 2–3 drops of glacial acetic acid was added. It was stirred for 6 h at room temperature. The yellow precipitate formed was filtered, washed with methanol (10 ml), and dried under reduced pressure.

All other members of the homologous series were prepared in a similar manner. The yield, IR, NMR, and elemental data for the compounds are summarized as follows.

*2.3.5 N-[4-(Hexyloxy)-2-Hydroxybenzylidene]-N′-(4-Hexyloxybenzylidene) Azine (**6a**).* Yield: 75%. FT-IR (KBr, cm^{-1}): 3433 (OH), 2921, 2852 (aliphatic C—H), 1624 (C=N), 1509, 1470 (Ph), 1307, 1250 (OPh), 1020 (N—N). ^{1}H NMR ($CDCl_3$, TMS) δ_H (ppm): 11.72 (s, 1H, —OH), 8.65 (s, 1H, $ROC_6H_3OHC\underline{H}{=}N$), 8.60 (s, 1H, $ROC_6H_4C\underline{H}{=}N$), 8.51–6.50 (m, 7H, ArH), 4.02–3.96 (t, 4H, $-O\underline{CH_2}$), 1.82–1.27 (m, 16H, $-[CH_2]_n$), 0.90–0.86 (t, 6H, $-CH_3$). ^{13}C NMR δ_c ($CDCl_3$): 163.5, 163.1 (CH=N), 161.8, 161.7, 161.5, 161.1 160.6 ($\underline{C}$—OH), 133.2 (Ar—C), 130.1, 130.0, 126.7, 114.7, 111.2, 107.6, 101.5, 77.4, 77.0, 76.5 ($CDCl_3$), 68.1 ($-OCH_2$), 31.8, 29.5, 29.3, 29.1, 29.0, 25.9, 22.6, 14.1 (CH_3). UV-visible ($CHCl_3$): $\lambda_{max} = 354, 330, 319, 304, 260$ nm. Elemental analyses: calculated for $C_{26}H_{36}N_2O_3$ (%): C, 73.55; H, 8.54; N, 6.59; found: C, 73.21; H, 8.32; N, 6.83.

*2.3.6 N-[4-(Heptyloxy)-2-Hydroxybenzylidene]-N′-(4-Hexyloxybenzylidene) Azine (**6b**).* Yield: 72%. FT-IR (KBr, cm^{-1}): 3432 (OH), 2921, 2852 (aliphatic C—H), 1621 (C=N), 1507, 1472 (Ph), 1307, 1251 (OPh), 1021 (N—N). ^{1}H NMR ($CDCl_3$, TMS) δ_H (ppm): 11.74 (s, 1H, —OH), 8.65 (s, 1H, $ROC_6H_3OHC\underline{H}{=}N$), 8.60 (s, 1H, $ROC_6H_4C\underline{H}{=}N$), 8.51–6.50 (m, 7H, ArH), 4.02–3.97 (t, 4H, $-OCH_2$), 1.82–1.27 (m, 20H, $-[CH_2]_n$), 0.90–0.86 (t, 6H, $-CH_3$). ^{13}C NMR δ_c ($CDCl_3$): 163.5, 163.1 (CH=N), 161.8, 161.7, 161.5, 161.1, 160.6 ($\underline{C}$—OH), 133.2 (Ar—C), 130.1, 130.0, 126.7, 114.7, 111.2, 107.6, 101.5, 77.4, 77.0, 76.5 ($CDCl_3$), 68.1 ($-OCH_2$), 31.8, 29.5, 29.3, 29.1, 29.0, 25.9, 22.6, 14.1 (CH_3). UV-visible ($CHCl_3$): $\lambda_{max} = 350, 338, 318, 308, 261$ nm. Elemental analyses: calculated for $C_{28}H_{40}N_2O_3$ (%): C, 74.30; H, 8.90; N, 6.18; found: C, 74.56; H, 8.81; N, 5.82.

*2.3.7 N-[4-(Decyloxy)-2-Hydroxybenzylidene]-N′-(4-Decyloxybenzylidene) Azine (**6c**).* Yield: 70%. FT-IR (KBr, cm^{-1}): 3433 (OH), 2921, 2852 (aliphatic C—H), 1626 (C=N), 1574, 1510 (Ph), 1301, 1250 (OPh), 1020 (N—N). ^{1}H NMR ($CDCl_3$, TMS) δ_H (ppm): 11.72 (s, 1H, —OH), 8.66 (s, 1H, $ROC_6H_3OHC\underline{H}{=}N$), 8.60 (s, 1H, $ROC_6H_4C\underline{H}{=}N$), 8.51–6.48 (m, 7H, ArH), 4.02–3.98 (t, 4H, $-OCH_2$), 1.84–1.34 (m, 32H, $-[CH_2]_n$), 0.93–0.91 (t, 6H, $-CH_3$). ^{13}C NMR δ_c ($CDCl_3$): 163.5, 163.1 (CH=N), 161.8, 161.7, 161.5, 161.1, 160.6 ($\underline{C}$—OH), 133.2 (Ar—C), 130.1, 130.0, 126.7, 114.7, 114.8, 111.2, 107.6, 101.5, 77.4, 77.0, 76.5 ($CDCl_3$), 68.1 ($-OCH_2$), 31.8, 29.5, 29.3, 29.1, 29.0, 25.9, 22.6, 14.1 (CH_3). UV-visible ($CHCl_3$): $\lambda_{max} = 386, 356, 332, 305, 257, 222$ nm. Elemental analyses: calculated for $C_{34}H_{52}N_2O_3$ (%): C, 76.07; H, 9.76; N, 5.21; found: C, 75.68; H, 9.48; N, 5.68.

*2.3.8 N-[4-(Dodecyloxy)-2-Hydroxybenzylidene]-N′-(4-Decyloxybenzylidene) Azine (**6d**).* Yield: 70%. FT-IR (KBr, cm^{-1}): 3428 (OH), 2920, 2861 (aliphatic C—H), 1628 (C=N), 1572, 1508 (Ph), 1301, 1252 (OPh), 1021 (N—N). ^{1}H NMR ($CDCl_3$, TMS) δ_H (ppm): 11.72 (s, 1H, —OH), 8.66 (s, 1H, $ROC_6H_3OHC\underline{H}{=}N$), 8.60 (s, 1H, $ROC_6H_4C\underline{H}{=}N$), 8.51–6.48 (m, 7H, ArH), 4.02–3.97 (t, 4H, $-OCH_2$), 1.84–1.34 (m, 40H, $-[CH_2]_n$), 0.93–0.86 (t, 6H, $-CH_3$). ^{13}C NMR δ_c ($CDCl_3$): 163.5, 163.1 (CH=N), 161.8, 161.7, 161.5, 161.1, 160.6 ($\underline{C}$—OH), 133.2 (Ar—C), 130.0, 126.7, 114.7, 111.2, 107.6, 101.5, 77.4, 77.0, 76.5 ($CDCl_3$), 68.1 ($-OCH_2$), 31.8, 29.5, 29.3, 29.1, 29.0, 25.9, 22.6, 14.1 (CH_3). UV-visible ($CHCl_3$): $\lambda_{max} = 353, 315, 302, 264, 205$ nm. Elemental analyses: calculated for $C_{38}H_{60}N_2O_3$ (%): C, 76.98; H, 10.19; N, 4.72; found: C, 76.52; H, 9.92; N, 4.39.

2.3.9 N-[4-(Tetradecyloxy)-2-Hydroxybenzylidene]-N′-(4-Decyloxybenzylidene) Azine (**6e**). Yield: 71%. FT-IR (KBr, cm^{-1}): 3428 (OH), 2922, 2852 (aliphatic C—H), 1627 (C=N), 1574, 1509 (Ph), 1301, 1252 (OPh), 1020 (N—N). ^{1}H NMR ($CDCl_3$, TMS) δ_H (ppm): 11.72 (s, 1H, —OH), 8.66 (s, 1H, $ROC_6H_3OHC\underline{H}{=}N$), 8.60 (s, 1H, $ROC_6H_4C\underline{H}{=}N$), 8.51–6.48 (m, 7H, ArH), 4.02–3.98 (t, 4H, $-OCH_2$), 1.84–1.34 (m, 48H, $-[CH_2]_n$), 0.93–0.86 (t, 6H, $-CH_3$). ^{13}C NMR δ_c ($CDCl_3$): 163.5, 163.1 (CH=N), 161.8, 161.5, 161.1, 160.6 ($\underline{C}$—OH), 133.2 (Ar—$\underline{C}$), 130.0, 126.7, 114.7, 111.2, 107.6, 101.5, 77.4, 77.0, 76.5 ($CDCl_3$), 68.1 ($-OCH_2$), 31.8, 29.5, 29.3, 29.1, 29.0, 25.9, 22.6, 14.1 (CH_3). UV-visible ($CHCl_3$): $\lambda_{max} = 353, 321, 279, 263, 208$ nm. Elemental analyses: calculated for $C_{42}H_{68}N_2O_3$ (%): C, 77.72; H, 10.56; N, 4.31; found: C, 77.49; H, 10.32; N, 4.24.

3. Synthesis of Copper (II) Complex of N-[4-(Decyloxy)-2-Hydroxybenzylidene]-N′-(4-Decyloxybenzylidene) Azine (7c)

To a solution of N-[4-(decyloxy)-2-hydroxybenzylidene]-N′-(4-decyloxybenzylidene) azine (**6c**) (2.14 g, 4 mmol) in chloroform (15 ml), a solution of copper (II) acetate (0.39 g, 2 mmol) in methanol was added and a brown precipitate was formed. The reaction mixture was stirred at room temperature for 1 h to complete the reaction. The precipitate was filtered off and washed with chloroform and methanol, respectively. The copper (II) complexes of all azines were prepared following the above procedure. These compounds were characterized by IR, NMR and UV-visible spectroscopy. The magnetic moment and analytical data are summarized below.

3.1 Bis-N-[4-(Hexyloxy)-2-Hydroxybenzylidene]-N′-(Hexyloxybenzylidene) Azine Copper (II) Complex, $C_{52}H_{70}N_4O_6Cu$ (7a)

Brown, yield: 65%. FT-IR (KBr, cm^{-1}): 2928, 2854 (aliphatic C—H), 1609 (C=N), 1573, 1511 (Ph), 1245 (OPh), 1024 (N—N). ^{1}H NMR ($CDCl_3$, TMS) δ_H (ppm): 8.60 (s, 4H, CH=N), 7.77–6.93 (m, 14H, ArH), 4.02–4.00 (t, 8H, $-OCH_2$), 1.82–1.27 (m, 32H, $-[CH_2]_n$), 0.90–0.86 (t, 12H, $-CH_3$). UV-visible (Nujol): $\lambda_{max} = 352, 326, 310, 298, 284, 268, 252, 210$ nm. $\mu_{eff} = 1.84$ BM. Elemental analyses: calculated for $C_{52}H_{70}N_4O_6Cu$ (%): C, 68.58; H, 7.74; N, 6.15; Cu, 6.97; found: C, 68.24; H, 7.38; N, 5.72; Cu, 6.71.

*3.1.1 Bis-N-[4-(Heptyloxy)-2-Hydroxybenzylidene]-N′-(Heptyloxybenzylidene) Azine Copper (II) Complex, $C_{56}H_{78}N_4O_6Cu$ (**7b**).* Brown, yield: 62%. FT-IR (KBr, cm^{-1}): 2921, 2859 (aliphatic C—H), 1610 (C=N), 1578, 1510 (Ph), 1249 (OPh), 1022 (N—N). ^{1}H NMR ($CDCl_3$, TMS) δ_H (ppm): 8.60 (s, 4H, CH=N), 7.77–6.93 (m, 14H, ArH), 4.02–3.98 (t, 8H, $-OCH_2$), 1.82–1.27 (m, 40H, $-[CH_2]_n$), 0.90–0.86 (t, 12H, $-CH_3$). UV-visible (Nujol): $\lambda_{max} = 378, 346, 321, 322, 297, 272, 252, 207$ nm. $\mu_{eff} = 1.82$ BM. Elemental analyses: calculated for $C_{56}H_{78}N_4O_6Cu$ (%): C, 69.57; H, 8.13; N, 5.79; Cu, 6.97; found: C, 69.81; H, 7.92; N, 5.38; Cu, 6.24.

*3.1.2 Bis-N-[4-(Decyloxy)-2-Hydroxybenzylidene]-N′-(Decyloxybenzylidene) Azine Copper (II) Complex, $C_{68}H_{102}N_4O_6Cu$ (**7c**).* Brown, yield: 67%. FT-IR (KBr, cm^{-1}): 2921, 2852 (aliphatic C—H), 1608 (C=N), 1573, 1511 (Ph), 1305, 1251 (OPh), 1023 (N—N). ^{1}H NMR ($CDCl_3$, TMS) δ_H (ppm): 8.60 (s, 4H, CH=N), 7.77–6.93 (m, 14H, ArH), 4.02–3.98 (t, 8H, $-OCH_2$), 1.82–1.27 (m, 64H, $-[CH_2]_n$), 0.90–0.86 (t, 12H, $-CH_3$). UV-visible (Nujol): $\lambda_{max} = 425, 346, 326, 298, 284, 268, 252, 210$ nm. $\mu_{eff} = 1.78$ BM. Elemental analyses: calculated for $C_{68}H_{102}N_4O_6Cu$ (%): C, 71.95; H, 9.05; N, 4.93; Cu, 5.59; found: C, 71.56; H, 8.68; N, 5.12; Cu, 5.34.

*3.1.3 Bis-N-[4-(Dodecyloxy)-2-Hydroxybenzylidene]-N′-(Dodecyloxybenzylidene) Azine Copper (II) Complex, $C_{76}H_{118}N_4O_6Cu$ (**7d**).* Brown, yield: 62%. FT-IR (KBr, cm^{-1}): 2931, 2849 (aliphatic C—H), 1610 (C=N), 1578, 1509 (Ph), 1302, 1250 (OPh), 1021 (N—N). ^{1}H NMR ($CDCl_3$, TMS) δ_H (ppm): 8.60 (s, 4H, CH=N), 7.77–6.93 (m, 14H, ArH), 4.02–3.98 (t, 8H, $-OCH_2$), 1.82–1.27 (m, 80H, $-[CH_2]_n$), 0.90–0.86 (t, 12H, $-CH_3$). UV-visible (Nujol): $\lambda_{max} = 382, 356, 345, 315, 298, 268, 251, 212$ nm. $\mu_{eff} = 1.74$ BM. Elemental analyses: calculated for $C_{76}H_{118}N_4O_6Cu$ (%): C, 73.18; H, 9.53; N, 4.49; Cu, 5.09; found: C, 73.54; H, 9.41; N, 3.95; Cu, 5.17.

*3.1.4 Bis-N-[4-(Tetradecyloxy)-2-Hydroxybenzylidene]-N′-(Tetradecyloxybenzylidene) Azine Copper (II) Complex, $C_{84}H_{134}N_4O_6Cu$ (**7e**).* Brown, yield: 69%. FT-IR (KBr, cm^{-1}): 2932, 2852 (aliphatic C—H), 1614 (C=N), 1574, 1512 (Ph), 1305, 1253 (OPh), 1024 (N—N). ^1H NMR ($CDCl_3$, TMS) δ_H (ppm): 8.60 (s, 4H, CH=N), 7.77–6.93 (m, 14H, ArH), 4.02–3.98 (t, 8H, —OCH_2), 1.82–1.27 (m, 96H, —$[CH_2]_n$), 0.90–0.86 (t, 12H, —CH_3). UV-visible (Nujol): λ_{max} = 372, 342, 290, 284, 262, 250, 208 nm. μ_{eff} = 1.72 BM. Elemental analyses: calculated for $C_{84}H_{134}N_4O_6Cu$ (%): C, 74.21; H, 9.93; N, 4.12; Cu, 4.67; found: C, 73.51; H, 9.43; N, 3.98; Cu, 4.51.

4. Results and Discussion

The synthetic routes for the preparation of the compounds N-[4-(alkoxy)-2-hydroxybenzylidene]-N’-(alkoxybenzylidene) azines (**6a–e**) and their copper (II) complexes (**7a–e**) are outlined in Scheme 1. The elemental analyses, FT-IR, and NMR spectra are fully consistent with the structures. The IR spectrum of 4-decyloxybenzhydrazone (**3c**) exhibits bands at 3381, 3284, 2934, 2861, 1632, 1601, 1505, 1308, 1260, and 1031 cm^{-1}, which are attributed to ν_a(N—H), ν_S(N—H), aliphatic C—H, ν(CH=N), ν(Ph), ν(OPh), and ν(N—N) modes, respectively. In the spectrum of N-[4-(decyloxy)-2-hydroxybenzylidene]-N′-(4-decyloxybenzylidene) azine (**6c**), bands appearing at 3433, (2921, 2852), 1626, (1574, 1510), (1301, 1250), and 1020 cm^{-1} are assigned to the ν(OH), ν(aliphatic C—H), ν(C=N), ν(Ph), ν(OPh), and ν(N—N) modes, respectively. In the IR spectrum of the copper complex of N-[4-(decyloxy)-2-hydroxybenzylidene]-N′-(4-decyloxybenzylidene) azine (**7c**), the ν(C=N) bands shift to a lower frequency (1608 cm^{-1}), indicating bonding through the azomethine nitrogen. The lowering in the frequency of ν(C=N) band caused by the coordination of the nitrogen to the metal center is in agreement with the result obtained for similar other complexes [11–16]. The bonding through the nitrogen of the azine to the Cu (II) ion is further supported by the shift of the ν(N—N) bond to a higher position (1023 cm^{-1}) compared with its position in the spectrum of the parent ligand (**6c**) at 1020 cm^{-1}. The increase in frequency of the ν(N—N) bond in the metal complex is due to a decrease in repulsion between the lone pairs of electrons on both the nitrogens.

The proton NMR spectrum of N-[4-(decyloxy)-2-hydroxybenzylidene]-N′-(4-decyloxybenzylidene) azine (**6c**) exhibits signals at δ 11.72 (s), 8.66 (s), 8.60 (s), 8.51–6.48 (m), 4.02–3.98 (t), 1.84–1.34 (m), and 0.93–0.91 (t), which are attributed to —OH, —CH=N of *o*-hydroxy-*p*-alkoxybenzylidene, —CH=N of *p*-alkoxybenzylidene, aromatic ring, —OCH_2, —$[CH_2]_n$, and —CH_3 protons, respectively. The major signals in the ^{13}C NMR spectrum of the compound (**6c**) are observed at δ 163.5, 160.6, 114.7, 68.1, 25.9, and 14.1, respectively, which are attributed to —CH=N, ortho —OH, aromatic ring, —OCH_2, —$OCH_2\underline{C}H_2$, and —CH_3 carbon, respectively.

The proton NMR spectrum of bis-N-[4-(decyloxy)-2-hydroxybenzylidene]-N′-(decyloxybenzylidene) azine copper (II) complex (**7c**) reveals signals at δ 8.60, 7.73–6.93, 4.02–3.98, 1.82–1.27, and 0.90–0.86, which are attributed to —CH=N of para-alkoxybenzylidene, aromatic ring, —OCH_2, —$[CH_2]_n$, and —CH_3 protons, respectively. The disappearance of the —OH signal from the spectrum of the metal complex indicates the deprotonation of the OH group and the resulting phenolate oxygen is bonded to the metal. The bonding of one of the azomethine nitrogens in proximity to the phenoxy oxygen would result in a downfield shift in the —CH=N signal and thus giving one signal at higher positions than that in the free azine and one signal due to the CH=N of alkoxy azine. However, only one signal is observed at the upfield (δ 8.60). The downfield shift in CH=N near copper may be counterbalanced by the upfield shift in the signal due to

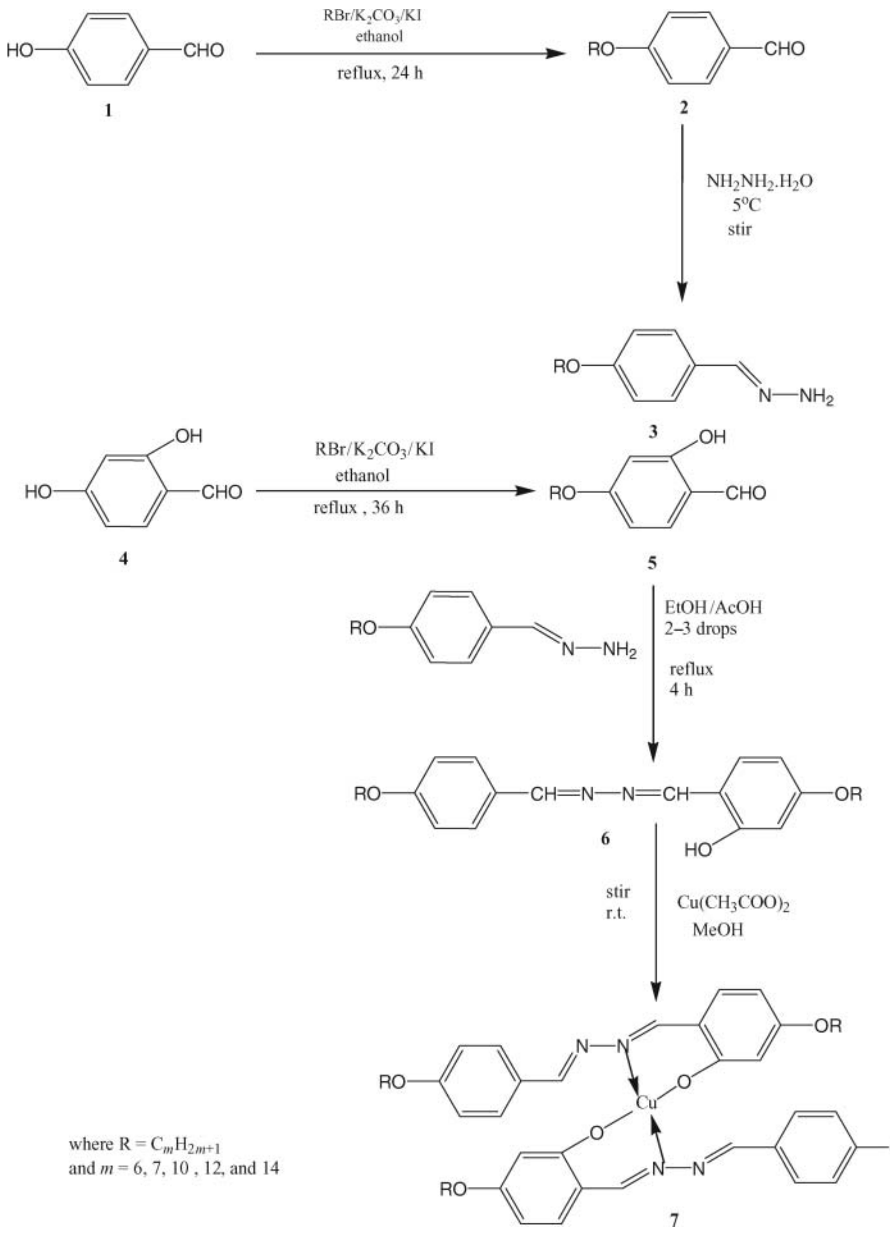

where R = C_mH_{2m+1}
and m = 6, 7, 10 , 12, and 14

Scheme 1. Route for the synthesis of N-[4(alkoxy)-2-hydroxybenzylidene]-N′-(4-alkoxy benzylidene) azines and their copper (II) complexes.

the delocalization of the unpaired d-electron in the chelate ring. Thus, only one signal is observed due to both types of CH=N protons. This phenomenon of the bonding effect of the metal ion, and the appearance of the sharp signal in the metal complex without line broadening, is similar to the unsymmetrical azines reported earlier and its reasoning has also been discussed earlier [17,18]. Based on these observations and elemental data, it is concluded that the unsymmetrical azine is bonded to the metal ion as a bidentate (N, O) ligand.

The electronic spectrum of N-[4-(decyloxy)-2-hydroxybenzylidene]-N′-(decyloxybenzyilidene) azine (**6c**) displays bands at 386, 356, 332, 305, 257, and 222 nm, which are assigned to n-π^* and π-π^* transitions. In the spectrum of the bis-N-[4-(decyloxy)-2-hydroxybenzylidene]-N’-(decyloxybenzylidene) azine copper (II) complex (**7c**), the UV bands are observed at 425, 346, 326, 298, 284, 262, 252, and 210 nm. The first band is characteristic of square planar coordination around the metal center [19]. The remaining bands are attributed to the π-π^* and n-π^* transitions of the ligand. The copper compounds exhibit magnetic moments at 1.72–1.84 BM, suggesting the presence of one unpaired electron.

5. Optical Properties

The liquid crystalline properties of N-[4-(alkoxy)-2-hydroxybenzylidene]-N′-(4-alkoxybenzylidene) azines **6a–e** and their copper (II) complexes were investigated by polarizing optical microscopy using a heating and cooling stage. The phase transition temperatures and enthalpies were measured by carrying out DSC thermal analyses. The Cr, SmA, N, and I denote crystalline, smectic A, nematic, and isotropic phases, respectively. The compound **6c** exhibited endothermic peaks at 68.5°C, 75.3°C, 84.2°C, 90.8°C, 104.3°C, 127.5°C, 133.7°C, 147.2°C, and 186.7°C as shown in Table 1. The endothermic peaks observed are the characteristic of crystal-to-crystal phase transition (polymorphism) with enthalpies of 0.4, 13.4, 3.3, 2.6, 9.8, 1.6, 0.8, 0.5, and 0.3 kJ mol^{-1}, but the peaks centered at 133.7°C ($\Delta H = 0.8$ kJ mol^{-1}), 147.2°C ($\Delta H = 0.5$ kJ mol^{-1}), and 186.7°C ($\Delta H = 0.3$ kJ mol^{-1}) define crystal-to-SmA, SmA-to-nematic, and nematic-to-isotropic phase transitions. The exothermic peak at 184.1°C ($\Delta H = 0.4$ kJ mol^{-1}) defines the isotropic-to-nematic phase transition, which further drifts to SmA centered at 144.1°C ($\Delta H = 0.5$ kJ mol^{-1}), followed by a crystal phase at 128.3°C ($\Delta H = 1.2$ kJ mol^{-1}), and then

Table 1. Transition temperatures (T) of the compound N-[4-(alkoxy)-2-hydroxy benzylidene]-N′-(4-alkoxybenzylidene) azine

Compounds	Transition temperatures (°C)
6a	Cr_1 138 I 105 N 100 Cr_1
6b	Cr 140 N 149 I 139 N 132 Cr
6c	Cr_1 68.5 (0.4)*(1.1)** Cr_2 75.3 (13.4) (38.4) Cr_3 84.2 (3.3) (9.2) Cr_4 90.8 (2.6) (7.1) Cr_5 104.3 (9.8) (25.9) Cr_6 127.5 (1.6) (4.1) Cr_7 133.7 (0.8) (3.9) SmA 147.2 (0.5) (1.1) N 186.7 (0.3) (0.6) I 184.1 (0.4) (0.8) N 144.1 (0.5) (1.1) SmA 128.3 (1.2) (2.6) Cr_7 123.3 (0.9) (2.5) Cr_6 104.4 (0.7) (1.9) Cr_5 95.4 (13.5) (36.6) Cr_4 78.2 (0.3) (0.8) Cr_3 70.6 (3.7) (10.4) Cr_2 44.7 (17.0) (53.5) Cr_1
6d	Cr_1 137 SmA I 135 SmA 115 Cr_1 110 Cr
6e	Cr_1 117 Cr_2 138 I 127 SmA 115 Cr_1 110 Cr

Note: Cr signifies crystal phase, SmA signifies smectic A phase, N signifies nematic phase, and I signifies isotropic liquid.

*The value in parentheses denotes enthalpy in kJ mol^{-1}.

**The value in parentheses denotes entropy in J K^{-1} mol^{-1}.

to successive polymorphic crystal phases. Thus, under optical microscopy, enantiotropic SmA and nematic mesophases were obtained for this compound. In the heating cycle, a transition from the crystal to the SmA phase appears at 133.7°C, which is texturally characterized by a focal-conic texture having a fluid property with higher viscosity exhibiting a stratified boundary with well-defined interlayer spacings. Further heating at 147.2°C shows the appearance of two to four black brushes emerging from the central nuclei forming disclination lines with a Schlieren texture showing the nematic mesophase. At 186.7°C, these nematic brushes disappear by forming bubbles and enter the isotropic phase of the heating cycle. In the cooling cycle, nematic droplets again appear at 184.1°C, which are slowly transformed into the SmA phase at 144.1°C and further drift to the crystal phase at 128.3°C. The crystal phase exhibits a diffuse transition to the successive crystal phase with characteristic polymorphism.

Under the optical microscope, compound **6d** exhibits a fluid property with dense viscosity and hexagonal pattern of an SmA phase at 137°C in the heating cycle drifting to the isotropic phase at 145°C. In the cooling cycle at 135°C, numerous droplets diffuse to the crystal phase at 115°C followed by the next sharp crystal phase transition at 110°C. This compound is characterized by a prominent enantiotropic SmA phase in both the heating and cooling cycles. The prominence of the SmA phase is due to the molecular packing, which is found to be random with additional intramolecular forces between the phenolic OH group and the nitrogen atoms in the unsymmetrical azines. Thus, a hexagonal array with a focal-conic texture is observed for this compound by optical microscopy, confirming the SmA phase. Moreover, it seems that strong core–core intermolecular interactions are present in the mesophase by means of hydrogen bonding between the hydroxyl groups. The asymmetrical azines reported by Centore et al. show both nematic and smectic phases [20,21].

Compound **6b** shows sudden nematic droplets in the heating cycle with a Schlieren texture at 140°C, which becomes an isotropic phase at 149°C. In the cooling cycle at 139.3°C, nematic droplets (bubbles) appear with a characteristic Schlieren texture (black stripes or black brushes) with surface defect centers (hedgehog type) and tilted alignment as four brushes are seen arising from the central nuclei. The mesophase drifts to the crystal phase at 132°C. Thus, the enantiotropic nematic phase is observed for this compound with the appearance of texture pattern in both the heating and cooling cycles.

Compound **6e** shows a fast crystal-to-crystal transition under the optical microscope at 117°C with a sharp transition to the isotropic phase at 138°C. In the cooling cycle, a sharp transition from the isotropic to the SmA phase, having a hexagonal array with focal-conic domains formed by deformed smectic layers that fold around two confocal line defects (preserving equidistance of structural layers everywhere except in the vicinity of the defect lines), is seen at 127°C. This transits slowly to an inconspicuous crystal phase at 120°C and finally to the next crystal phase at 113°C. Finally, compound **6a** exhibits no optical texture in the heating cycle and reaches the clearing temperatures at 138°C. In the cooling cycle, some nematic droplets appear and immediately cause crystallization at 105°C, followed by the next crystal phase at 100°C.

The compounds of the series N-[4-(alkoxy)-2-hydroxybenzylidene]-N′-(4-alkoxybenzylidene) azines **6a–e** exhibit both enantiotropic nematic and SmA mesophases in which the nematic phase is dominated by the SmA phase in the higher homologs of the series. Presumably, as strong core–core intermolecular interactions are present in the mesophase by means of hydrogen bonding between the hydroxyl group or with the nitrogen atom of the unsymmetrical azine in homologs with $m = 10$, 12, and 14, which promotes the occurrence of SmA phase. Thus, with an increase in the alkoxy chain length, the van der Waals forces increase, which alters the molecular packing and adds to the intermolecular forces between the hydroxyl group and the nitrogen atom of the unsymmetrical azine favoring the SmA phase in the higher homologs of the series.

The metal complexes of N-[4-(alkoxy)-2-hydroxybenzylidene]-N′-(4-alkoxy benzylidene) azines **7a–e** were found to be nonmesogenic with prominent polymorphic crystal phases exhibited in both cycles. The nonmesogenic property of the metal complexes is likely due to the symmetrical and rigid geometry of the metal complexes along with the stronger interaction of the potential donor (C=N) with the metal ion in the neighboring layers, resulting in packing of the molecules in the solid state. This result can be compared with our previous work [22] on metal-combining unsymmetrical azines. Although the basic unsymmetrical azines [22] displayed the dominant SmA phase, with a monotropic nematic phase in the $m = 8$ homolog. However, in this article, where we observe both enantiotropic nematic and smectic phases in some homologs of the series of the unsymmetrical N-[4-(alkoxy)-2-hydroxybenzylidene]-N′-(4-alkoxybenzylidene) azines, although in the higher homologs, the nematic phase is suppressed and the SmA phase dominates.

6. Conclusions

A new series of mesogenic unsymmetrical azines, N-[4-(alkoxy)-2-hydroxybenzylidene]-N′-(4-alkoxybenzylidene) azines, having terminal alkoxy chains ($m = 6 \sim 14$) and their copper (II) complexes have been synthesized. The structural elucidation of the final products was investigated by FT-IR, UV-visible spectroscopy, ^{1}H and ^{13}C NMR spectra, and magnetic susceptibility measurements. The transition enthalpy and entropy were characterized by DSC. The existence of the nematic and SmA phases was confirmed by polarizing optical microscopy. It was found that the unsymmetrical azines show mesomorphic properties, whereas their copper (II) complexes were nonmesogenic in nature and showed high melting points of ∼240°C.

Acknowledgments

The authors thank the Head of the Department of Chemistry, Banaras Hindu University (BHU), Varanasi, for providing laboratory facilities. Ashwini Pandey thanks the Council of Scientific and Industrial Research (CSIR, New Delhi) for financial support as senior research fellow at BHU, Varanasi. Thanks are also due to the staff of analytical division for CHN analyses, and for ^{1}H, ^{13}C NMR, IR, and electronic spectra.

References

[1] Yang, Z., Zheng, J., & Yang, C. (2004). *Lanz. Univ., J. Sichuan Union Univ., Eng. Sci .Ed.*, *40*, 51.

[2] Hoelzemann, G. (2006). *Expert Opin. Ther. Pat.*, *16*, 1175.

[3] Dragancea, D., Arion, V. B., & Shova, S. (2005). *Angew. Chem: Int Ed. Engl.*, *44*, 7938.

[4] Rajeswaran, M., Blanton, T. N., & Giesen, D. J. (2006). *J. Solid State Chem.*, *179*, 1053.

[5] Hashidzume, A., Tsuchiya, A., & Morishima, Y. (2000). *Macromolecules*, *33*, 2395.

[6] Takahashi, H., Kubo, K., Takechi, H., & Matsumoto, T. (2006). *J. Oleo. Sci.*, *55*, 483.

[7] Iwan, A., Rannou, P., Janeczek, H., Palewicz, M., Hreniak, A., Bilski, P., Oswald, F., & Pociecha, D. (2010). *Synthetic Metals*, *160*, 859.

[8] Singh, B., & Pandey, A. (2010). *Mol. Cryst. Liq. Cryst.*, *517*, 148.

[9] Singh, B., & Pandey, A. (2010). *Liq. Cryst.*, *37*, 57.

[10] Singh, B., & Pandey, A. (2010). *Liq. Cryst.*, *37*, 58.

[11] Khandar, A. A., & Rezvani, Z. (1998). *Polyhedron*, *18*, 129.

[12] Rezvani, Z., Ahar, R., Nejati, K., & Seyedahamian, S. M. (2010). *Acta Chim. Slov.*, *51*, 675.

[13] Rezvani, Z., Abbasi, A. R., Nejati, K., & Seyedahamian, S. M. (2005). *Polyhedron*, *24*, 1461.

[14] Rezvani, Z., Divband, B., Abbasi, A. R., & Nejati, K. (2006). *Polyhedron*, *25*, 1915.

[15] Lee, M., Yoo, Y. S., & Chol, M. G. (1999). *Macromolecules*, *32*, 2777.

[16] Singh, B., & Pandey, A. (2010). *Liq. Cryst.*, *37*, 64.

[17] Shaw, D. (1976). *Fourier Transform NMR Spectroscopy*—Varian Associates Ltd., Walton-on Thames; Elsevier Scientific Publishing Company: New York, Chapter 8, p. 203.

[18] Eaton, D. R., & Philips, W. D. (1965). *Adv. Magn. Res.*, *4*, 103.

[19] Temel, H., Ilhan, S., Sekerci, M., & Ziyadanogullari, R. (2002). *Spectr. Lett.*, *35*, 219.

[20] Centore, R., & Garzillo, C. (1997). *J. Chem. Soc. Perkin Trans.*, *2*, 79.

[21] Centore, R., Panunzi, B., Roviello, A., Sirigu, A., & Villano, P. (1996). *Mol. Cryst. Liq. Cryst.*, *275*, 107.

[22] Singh, B., & Pandey, A. (2010). *Liq. Cryst.*, *37*, 66.